

RSC Advances



This is an *Accepted Manuscript*, which has been through the Royal Society of Chemistry peer review process and has been accepted for publication.

Accepted Manuscripts are published online shortly after acceptance, before technical editing, formatting and proof reading. Using this free service, authors can make their results available to the community, in citable form, before we publish the edited article. This *Accepted Manuscript* will be replaced by the edited, formatted and paginated article as soon as this is available.

You can find more information about *Accepted Manuscripts* in the [Information for Authors](#).

Please note that technical editing may introduce minor changes to the text and/or graphics, which may alter content. The journal's standard [Terms & Conditions](#) and the [Ethical guidelines](#) still apply. In no event shall the Royal Society of Chemistry be held responsible for any errors or omissions in this *Accepted Manuscript* or any consequences arising from the use of any information it contains.

1 **Facile synthesis of chitosan-capped ZnS quantum dots as an**
2 **eco-friendly fluorescence sensor for rapid determination of**
3 **bisphenol A in water and plastic samples**

4 Xianyi Cao¹, Fei Shen¹, Minwei Zhang, Jiabin Bie, Xin Liu, Yeli Luo, Jijia Guo, Chunyan Sun*

5 Department of Food Quality and Safety, College of Quartermaster Technology, Jilin University, Changchun
6 130062, China

7 **Abstract**

8 The paper described a novel eco-friendly fluorescence sensor for determination of bisphenol
9 A (BPA) based on chitosan-capped ZnS quantum dots (QDs). By using safe and inexpensive
10 materials, nontoxic ZnS QDs were synthesized via an environment-friendly method using chitosan
11 as capping agent. The as-prepared ZnS QDs exhibited characteristic absorption (absorbance edge
12 at 310 nm) and emission (maxima at 430 nm) spectra with a relatively high fluorescence quantum
13 yield of 11.8%. Quantitative detection of BPA was developed based on fluorescence quenching of
14 chitosan-capped ZnS QDs with high sensitivity and selectivity. Under the optimal conditions, the
15 fluorescence response of ZnS QDs was linearly proportional to BPA concentration in a wide range
16 from 0.50 to 300 $\mu\text{g}\cdot\text{L}^{-1}$ with a detection limit of 0.08 $\mu\text{g}\cdot\text{L}^{-1}$. Most of potential coexisting
17 substances did not interfere with the BPA-induced quenching effect. The proposed analytical
18 method for BPA was successfully applied to water and plastic real samples, and the possible
19 quenching mechanism was also discussed.

20 **Key words:** Bisphenol A, Zinc sulfide, Quantum dots, Sensor, Chitosan, Fluorescence quenching

21

* Corresponding author. Tel.: +86 431 87836375; fax: +86 431 87836391 (C. Sun)

E-mail addresses: sunchunyan1977@163.com, sunchunyan@jlu.edu.cn (C. Sun)

¹First two authors contributed equally to this work.

22 1. Introduction

23 Bisphenol A (BPA), 2,2-bis(4-hydroxyphenyl) propane, is one of the most important
24 chemical raw materials in the world.¹ It is synthesized by phenol and acetone under catalysis of
25 acid or base, and widely used for the production of polycarbonate (PC) and epoxy resins (EP),
26 along with other applications. Among their uses, a wide variety of food contact materials are
27 noticeable, such as tableware, storage container, water pipe, infant feeding bottle and protective
28 lining for beverage cans.² Because of BPA's high volume production and widespread use in
29 human life, however, there is far-ranging environmental contamination and human exposure to
30 BPA.³ Its presence in food has been paid great attention since it composes the principal pathway
31 of human exposure.⁴ Because of incomplete polymerization and degradation of the polymers
32 under high temperature, BPA can migrate from food contact materials to food or water.⁵ As an
33 exogenous endocrine disrupting chemical (EDC), endocrine disrupting activity of BPA has a
34 considerably negative impact on human health. Exposure to BPA might be an important factor in
35 the decreasing sperm count in males, the increasing rates of mammary cancer, the increase in other
36 diseases linked to endocrine dyscrasia, as well as the increase of neural and behavioral changes in
37 infants and children.^{6,7} Thus there is an urgent need to monitor the presence of BPA in daily water
38 correlated to BPA-based food contact materials.

39 Traditional detection methods for BPA such as high performance liquid chromatography
40 (HPLC),⁸ liquid chromatography/mass spectrometry (LC/MS),⁹ gas chromatography/mass
41 spectrometry (GC/MS),¹⁰ enzyme-linked immunosorbent assay (ELISA)¹¹ and capillary
42 electrophoresis (CE),¹² require expensive instrumentation, considerable time, experienced
43 technician and complex sample pretreatment, so their application in on-site rapid analysis is

44 extremely limited. Recently, different types of analytical methods including electrochemistry,¹³
45 chemiluminescence,¹⁴ quartz crystal microbalance (QCM),¹⁵ aptasensor-based colorimetric
46 method with Au nanoparticles,¹⁶ surface plasmon resonance (SPR) biosensor,¹⁷ liposome
47 chromatography¹⁸ *etc.*, have been developed to determine BPA, but most of them suffer from
48 complex chemical synthesis, the use of volatile organic solvents, high cost or poor sensitivity.
49 Therefore, developing rapid, simple, sensitive, low-cost and eco-friendly methods for BPA
50 detection has become very essential.

51 Fluorescence assay is a promising analytical technique with the advantage of less sample,
52 low cost, high sensitivity, quick-response and easy operation. Thus, in recent years, it is widely
53 used in biochemical, food and environmental science. There have been several reports on
54 fluorescence determination for BPA,¹⁹⁻²¹ and the detection limits are comparable with those of
55 HPLC,⁸ LC/MS⁹ and GC/MS,¹⁰ and approximately 1-3 orders of magnitude lower than those
56 reported by other methods such as ELISA,¹¹ CE,¹² electrochemistry¹³ and chemiluminescence.¹⁴
57 BPA can give a fluorescence signal by itself as its molecule possesses a conjugated cyclic
58 structure, but in aqueous solution the signal is so weak that direct determination can only obtain a
59 poor detection performance.²² Some fluorescent probes are utilized for detection of BPA, such as
60 fluorescent dyes,¹⁹ CdSe²⁰ and CdTe²¹ quantum dots (QDs). However, most of fluorescent dyes
61 have disadvantages of low photobleaching threshold, poor chemical stability and biocompatibility,
62 and Cd/Se/Te-based QDs have been confirmed to exhibit a strong cytotoxic activity.²³ Thus,
63 Zn-based QDs may be regarded as a promising new choice of nanophosphors for detection of BPA,
64 as they are a type of nontoxic (or low-toxic) QDs compared with traditional Cd/Se/Te-based
65 QDs.²⁴ To the best of our knowledge, there is no report on fluorescence detection for BPA with

66 Zn-based QDs. Chitosan, β -(1,4)-2-amino-2-deoxy-D-glucose, is a unique cationic biocompatible
67 polysaccharide built by repeated units of N-acetyl-D-glucosamine and D-glucosamine, derived
68 from the partial deacetylation of chitin, a natural polysaccharide extracted from the crustacean
69 shells. Chitosan exhibits a desirable chelating ability with transition metal ions due to its special
70 structure, which makes it possible for its metal ion complexes to be used as precursors to
71 synthesize QDs. Moreover, its high viscosity can effectively prevent the aggregation of QDs,
72 which will greatly enhance the stability of QDs in aqueous solution.²⁵

73 Herein, we present a novel eco-friendly fluorescence sensor for detection of BPA based on
74 chitosan-capped ZnS QDs. Chitosan was used as modifier as well as stabilizer, and well-dispersed
75 ZnS QDs with a uniform size were synthesized. By controlling the reaction conditions, the
76 fluorescent properties of chitosan-capped ZnS QDs could be well regulated. The obtained
77 water-soluble QDs were around 1.8 nm in diameter and displayed excellent fluorescent properties.
78 We investigated the interaction between chitosan-capped ZnS QDs and BPA in aqueous solution.
79 It was found that BPA dramatically quenched the fluorescence of chitosan-capped ZnS QDs, and
80 the change of fluorescence intensity was proportional to the concentration of BPA. Based on this
81 phenomenon, a sensitive, simple, rapid, low cost and environment-friendly fluorescence method
82 has been established for detection of BPA. Interference tests showed that some potential
83 co-existing substances, such as common inorganic ions and natural small molecules have little
84 interference. The possible mechanism of the proposed sensing method for BPA is also discussed
85 (Scheme 1). This green method has been applied to the determination of BPA content in water and
86 plastic samples and satisfactory results were obtained.

87 **2. Experimental**

88 2.1 Chemicals, materials and apparatus

89 All chemicals were of analytical grade and used as received without further purification.
90 High purity nitrogen (99.999%) and double deionized water (DDW) were used in all experiments.
91 Zinc acetate [$\text{Zn}(\text{CH}_3\text{COO})_2 \cdot 2\text{H}_2\text{O}$], sodium sulfide ($\text{Na}_2\text{S} \cdot 9\text{H}_2\text{O}$) and acetic acid were purchased
92 from Xilong Chemical Co., Ltd (Shantou, Guangdong, China). Chitosan (high molecular weight, \geq
93 75% deacetylated) and BPA were purchased from Sigma-Aldrich (St. Louis, Missouri, USA).
94 CaCl_2 , NaCl , NH_4Cl , MgCl_2 , MnCl_2 , CuCl_2 , AlCl_3 , FeCl_3 , ZnCl_2 , BaCl_2 , KNO_3 , Na_3PO_4 , Na_2SO_4 ,
95 Na_2CO_3 , AgNO_3 , $\text{Hg}(\text{NO}_3)_2$, NaOH , CH_3COONa , HCl , glucose, lactose and glycine were
96 purchased from Beijing Chemical Reagent Company (Beijing, China). Rhodamine 6G (Rh 6G)
97 was obtained from Sinopharm Chemical Reagent Co., Ltd (Shanghai, China). Different brands of
98 packaged drinking water, plastic cups, feeding bottles, microwave lunch boxes and epoxy
99 resin-based bowls were procured from a local market. Besides, tap and rain water was also
100 collected in our laboratory and campus, respectively.

101 The absorption spectra were recorded on a 2550 UV-vis spectrophotometer (Shimadzu,
102 Tokyo, Japan). The fluorescence spectra were obtained on a RF-5301PC fluorescence
103 spectrophotometer (Shimadzu, Tokyo, Japan) with both of the exciting and emission slits set at 5
104 nm. High resolution transmission electron microscopy (HRTEM) measurements were made on a
105 TECNAI F20 (FEI Co., Eindhoven, Netherlands) operated at an accelerating voltage of 200 kV. A
106 drop of the QDs solution was drop-cast on ultra-thin carbon film-supported copper grids and
107 subsequently air-dried before HRTEM analysis. FT-IR spectra were recorded with an
108 IRPrestige-21 FT-IR spectrometer (Shimadzu, Tokyo, Japan). Zeta potential was obtained on a
109 Zetasizer Nano ZS90 particle size analyzer (Malvern, Worcestershire, UK). The ultrasonic

110 treatment was carried out on a 125 KQ-300DE ultrasonicator (Kunshan, Shanghai, China). The
111 centrifugation was performed on a CR20B2 refrigerated centrifuge (Hitachi, Tokyo, Japan).
112 Magnetic stirring was carried out on a GL-3250B magnetic stirrer (QILINBEIER, Haimen, China).
113 All pH measurements were carried out with a Model pHS-3C pH meter (Chenghua, Shanghai,
114 China). All optical measurements were performed at room temperature under ambient conditions.

115 **2.2 Synthesis and purification of water-soluble chitosan-capped ZnS QDs**

116 Chitosan is nearly insoluble in strong acidic and neutral media but soluble in weak acidic
117 media, as amine group is protonated to NH_3^+ ,²⁶ thus we used 1% (v/v) acetic acid aqueous solution
118 to dissolve chitosan. Water-soluble chitosan-capped ZnS QDs were synthesized according to the
119 procedure described previously with some modification.^{26,27} 0.22 g of $\text{Zn}(\text{CH}_3\text{COO})_2 \cdot 2\text{H}_2\text{O}$ was
120 firstly added to 99 mL of 0.05% (w/v) chitosan solution under constant stirring and heated at 80 °C
121 for 20 min to facilitate a chelating balance. After the solution naturally cooled down to room
122 temperature, 0.24 g of $\text{Na}_2\text{S} \cdot 9\text{H}_2\text{O}$ was dissolved in 1 mL of ice water and thereupon added
123 dropwise to the solution in an ice bath under continuous stirring and protection of N_2 . The molar
124 ratio of $\text{Zn}^{2+}:\text{S}^{2-}$ is 1.5:1. The addition of Na_2S resulted in the formation of a milky white
125 suspension immediately, and the solution was constantly stirred for 100 min. Then the solution
126 containing chitosan-capped ZnS QDs was centrifuged at 12000 rpm for 10 min. The precipitated
127 particles were washed 3 times using DDW and 0.1% (v/v) acetic acid aqueous solution
128 respectively to remove the adhered impurities and excess chitosan. The washed chitosan-capped
129 ZnS QDs were dried by a vacuum oven at 60 °C for 24 h. Finally, the prepared QDs were
130 dispersed in 100 mL 1% (v/v) acetic acid aqueous solution again and stored in a refrigerator at
131 4 °C for further use. The QDs suspension can keep clear without any sedimentation for months.

132 To obtain high-quality chitosan-capped ZnS QDs, the influences of different synthesis
133 conditions including the concentration of Zn^{2+} and chitosan, the molar ratio of $\text{Zn}^{2+}:\text{S}^{2-}$ and the
134 reaction time on the fluorescence intensity of ZnS QDs were investigated. According to the
135 evaluation for the above conditions, the concentration of Zn^{2+} and chitosan, the molar ratio of
136 $\text{Zn}^{2+}:\text{S}^{2-}$ and the reaction time were optimized to be $1.0 \times 10^{-4} \text{ mol}\cdot\text{L}^{-1}$, $0.50 \text{ g}\cdot\text{L}^{-1}$, 1.5:1 and 100
137 min, respectively. Under this synthesis condition, the as-prepared ZnS QDs can exhibit relatively
138 high fluorescence emission intensity and good analytical performance for detection of BPA.

139 **2.3 Analytical Procedure**

140 Typically, in a 5 mL test tube, a certain volume of $500 \mu\text{g}\cdot\text{L}^{-1}$ BPA aqueous solution was
141 added and the solution was diluted to 2 mL with DDW. Then the solution was mixed with 1 mL of
142 $3.5 \times 10^{-6} \text{ mol}\cdot\text{L}^{-1}$ chitosan-capped ZnS QDs. After the mixture was homogenized thoroughly and
143 equilibrated for 4.0 min at room temperature, the fluorescent intensity was recorded at excitation
144 wavelength of 315 nm. The calibration curve for BPA was established according to the ratio of
145 fluorescence intensity, that is, F_0/F , and F_0 and F are the maximum emission intensities of ZnS
146 QDs in the absence and presence of certain concentrations of BPA, respectively.

147 **2.4 Detection of BPA in real samples**

148 Tap and packaged drinking water were directly determined for the presence of BPA without
149 any pretreatment. Rain water was filtered with a $0.45 \mu\text{m}$ -filter membrane to remove particulate
150 matter.

151 According to Chinese National Standard GB/T 23296.1-2009 (Materials and articles in
152 contact with foodstuffs-Plastics substances subject to limitation-Guide to test methods for the
153 specific migration of substances from plastics to foods and food simulants and the determination

154 of substances in plastics and the selection of conditions of exposure to food simulants), contacting
155 temperature and time for the specific migrant test of BPA from plastic cup and feeding bottle to
156 water-based food or food simulant should be chosen as 100 °C (or reflux temperature) and 240
157 min. In order to shorten the pretreatment time for rapid detection of these plastic samples,
158 ultrasonic and microwave extraction were respectively chosen and applied in our experiments
159 according to the actual usages of the samples. An ultrasonicator (220 V, 200 W) and a microwave
160 oven (220 V, 500 W) were used in the extraction procedures. Plastic cups, feeding bottles,
161 microwave lunch boxes and epoxy resin-based bowls were washed with DDW thoroughly,
162 solarized and cut into small fragments about 5 mm × 5 mm size, respectively. Next, 10 g (± 0.0001
163 g) of each plastic sample was put into a conical beaker and 100 mL of DDW was added. The
164 solutions containing plastic cup or feeding bottle fragments were ultrasonic-extracted for 90 min
165 in a water bath (90 ± 0.5 °C). The solutions containing microwave lunch box or epoxy resin-based
166 bowl fragments were microwave-heated for 10 min. Then all the sample leaching solutions were
167 cooled to room temperature, filtered with a 0.45 µm-filter membrane and rediluted to 100 mL with
168 DDW. Finally, 1 mL of the water or plastic leaching solution samples was used for BPA
169 determination according to the proposed method in *Section 2.3*. In order to investigate the
170 recoveries of these water and plastic leaching solution samples, a certain amount of BPA was
171 doped into these samples, then pretreated and analyzed in accordance with the above procedure.

172 **3. Results and Discussion**

173 **3.1 Characteristics of chitosan-capped ZnS QDs**

174 Due to the protonation of -NH₂ group of chitosan in weak acidic condition, the surface of
175 chitosan-capped ZnS QDs possesses positive charges, which is supported by the zeta potential

176 data of the QDs suspension (Fig. S1A). The zeta potential of ZnS QDs was measured to be 40.4
177 mV, which indicates that the surface of ZnS QDs is strongly positive-charged. The QDs
178 suspension can be effectively stabilized against aggregation via electrostatic repulsion against van
179 der Waals attraction.

180 In order to identify the conjugation mode between ZnS QDs and chitosan, FT-IR
181 spectroscopy was applied to this study. The FT-IR spectra of pure chitosan (A) and
182 chitosan-capped ZnS QDs (B) are shown in Fig. 1, and the major characteristic peaks observed in
183 both spectra are shown in Table S1. The similarity in both spectral characteristics and major peak
184 positions indicates that chitosan was well chemically bound onto the surface of the ZnS QDs.
185 Moreover, by discerning the fine differences between the two spectra, the conjugation mode of
186 chitosan and ZnS QDs can be confirmed. It is important to note that the peak around 3300-3500
187 cm^{-1} corresponding to stretching vibrations of hydroxyl, amino and amide groups, moved to lower
188 wavenumber and became broader and stronger, which represents the strong interaction between
189 these groups and ZnS QDs. The mechanism of this interaction may be mainly due to hydrogen and
190 coordinate bonding, as the ZnS QDs growing in aqueous solution have a large amount of H_2O and
191 excess Zn^{2+} bound to the surface of the nanocrystallite, which interact with $-\text{OH}$ and $-\text{NH}_2$ of
192 chitosan via hydrogen and coordinate bond. This interaction will result in some other fine spectral
193 changes of covalent bonds in chitosan, especially for those corresponding to Zn^{2+} -bonded atoms.
194 Generally, coordination to metallic ions will reduce the electron density of metallic ions-bonded
195 atoms which makes stretching require less energy, and increase steric hindrance of covalent bonds
196 corresponding to metallic ions-bonded atoms which makes bending require more energy.
197 Therefore, the coordination between Zn^{2+} and chitosan caused the stretching vibration peaks of

198 covalent bonds corresponding to Zn^{2+} -bonded atoms shifting to lower wavenumber and their
199 bending vibration peaks moving to high wavenumber. In Fig. 1, the peaks located at 1264 and
200 1090 cm^{-1} respectively assigned to $\text{C}_2\text{-H}$ and $\text{C}_3\text{-O}$ stretching shifted to lower wavenumber 1261
201 and 1083 cm^{-1} , and the peak located at 1602 cm^{-1} assigned to N-H bending moved to a higher
202 wavenumber 1611 cm^{-1} , while the peak located at 1035 cm^{-1} attributed to $\text{C}_6\text{-O}$ stretching
203 remained stable. These changes show that N_2 and O_3 of chitosan molecule are more responsible
204 for the interaction with ZnS QDs and O_6 takes little part in the interaction. Other peak changes in
205 Table S1 can also confirm the above inference. Since the growth of ZnS QDs is almost *in situ*, we
206 may deduce that the complex sites between chitosan and ZnS QDs are mainly located at C_2 and C_3
207 of the chitosan repeating units. The inferred formation process of chitosan-capped ZnS QDs was
208 shown in Scheme 1C.

209 The chitosan-capped ZnS QDs are optically characterized by UV-vis absorption spectroscopy
210 and fluorometry. The normalized absorption (a) and fluorescence emission (b) spectra are shown
211 in Fig. 2A. The absorption edge of ZnS QDs is around 310 nm with a considerable blue-shift
212 compared to that of bulk ZnS at 340 nm ,²⁸ showing an apparent quantum confinement effect. The
213 emission maxima centered at 430 nm with the excitation of 315 nm. Photographs of the ZnS QDs
214 solution under daylight and a 308 nm UV lamp are respectively shown as c and d in Fig. 2A.
215 Under a 308 nm UV lamp, the QDs solution displayed bright blue fluorescence which was
216 attributed to the defect-related emission of ZnS. Besides, the fluorescence spectrum band is
217 relatively narrow and symmetric with full widths at half-maximum (FWHM) about 85 nm, which
218 reveals that the as-prepared QDs possess fairly uniform particle size due to their relatively low
219 size distribution.²⁹ The molar extinction coefficient (ϵ) of the chitosan-capped ZnS QDs at 315 nm

220 was estimated to be about $3.3 \times 10^5 \text{ M}^{-1} \cdot \text{cm}^{-1}$,²⁷ thus the molar concentration of the ZnS QDs was
221 calculated to be nearly $3.5 \times 10^{-6} \text{ mol} \cdot \text{L}^{-1}$ according to Lambert Beer's law. TEM is also performed
222 to study the morphology of the as-prepared chitosan-capped ZnS QDs. Fig. 2B shows a typical
223 image of the obtained ZnS QDs. The shape of these nanoparticles is close to spherical and partly
224 aggregated, with diameters ranging from 1.5 to 2.0 nm. The average particle size was about 1.8
225 nm.

226 Fluorescence quantum yield (QY) represents the efficiency of a fluorescent material in
227 converting the excitation into fluorescent emission. According to Williams' method,³⁰ by using Rh
228 6G (QY = 95%, in ethanol) as the reference and exciting all the samples at 315 nm, the QY of
229 chitosan-capped ZnS QDs was calculated from the following equation:

$$230 \quad \text{QY}_{\text{ZnS}} = \text{QY}_{\text{Rh 6G}} \cdot \frac{m_{\text{ZnS}}}{m_{\text{Rh 6G}}} \cdot \left(\frac{\eta_{\text{water}}}{\eta_{\text{ethanol}}} \right)^2 \quad (1)$$

231 where m and η are the slope of the integrated fluorescence intensity versus absorbance at 315 nm
232 and refractive index of the solvent respectively. The integrated fluorescence intensity was obtained
233 by integrating the emission intensity over the entire wavelength range under the emission peak,
234 and the absorbance was kept between 0.01 and 0.1 to avoid the self-absorption effect. With the
235 QY of Rh 6G taken as 95%, we obtained the QY of the ZnS QDs as 11.8%. Since it has been
236 widely accepted that the QDs whose QY is more than 10% can be considered for practical
237 applications,³¹ it could be concluded that the obtained ZnS QDs can show a satisfactory
238 fluorescent analytical performance in this assay.

239 3.2 Effects of BPA on the fluorescence of chitosan-capped ZnS QDs

240 According to the analytical procedure introduced in *Section 2.3*, the fluorescence emission
241 spectra of the as-prepared chitosan-capped ZnS QDs (Fig. 3) in the absence (a) and presence (b) of

242 BPA were recorded. The fluorescence band of chitosan-capped ZnS QDs was centered at 430 nm.
243 When BPA was added to the ZnS QDs solution, significant quenching of fluorescence intensity
244 was observed. In order to identify the origins of the fluorescence quenching, control experiments
245 were performed. Free ZnCl₂, chitosan and Zn²⁺-chitosan complex with the same concentrations as
246 those used in the synthesis of ZnS QDs were added into the mixture solution of ZnS QDs and
247 BPA. The obtained results revealed that these substances had no contribution to the quenching
248 effect of BPA on the fluorescence emission of ZnS QDs. Thus, the quenching effect was attributed
249 to the interaction between BPA and chitosan-capped ZnS QDs. Considering this remarkable
250 quenching of fluorescence intensity, the possibility of developing a simple and sensitive
251 fluorescence chemosensor for rapid detection of BPA should be further studied.

252 3.3 Optimization of assay conditions

253 The influence of reaction time on the fluorescence intensity of the system was investigated at
254 room temperature. The optimum incubation time for the reaction between ZnS QDs and BPA
255 reaching equilibrium was examined by recording the fluorescence spectra every 0.5 min at real
256 time (Fig. 4A). The results show that after addition of BPA into the ZnS QDs solution the
257 fluorescence intensity decreased by prolonging the reaction time and the equilibrium was obtained
258 within 4.0 min. F_0/F was nearly constant after 4.0 min and the fluorescence intensity of the
259 BPA-ZnS QDs system could keep stable for at least 50 min. Thus the reaction time was fixed at
260 4.0 min.

261 It is well known that fluorescence intensity of QDs is greatly affected by medium pH. Using
262 0.1 mol·L⁻¹ NaOH or 0.1 mol·L⁻¹ HCl for pH adjustment, the effects of the solution pH on the
263 fluorescence intensity of ZnS QDs in the absence and presence of BPA were investigated and the

264 results are shown in Fig. 4B and 3C respectively. In Fig. 4B, it can be seen that stable and high
265 fluorescence intensity was obtained in the pH range of 4.0-4.5 and pH lower than 4.0 or higher
266 than 4.5 resulted in a significant decrease of fluorescence intensity. Under the condition of pH <
267 4.0, the low fluorescence intensity is the result of dissociation of the QDs, as the interaction
268 between chitosan and ZnS QDs was wrecked and the stability of the QDs dramatically decreased.
269 With the increase of pH, the deprotonation of $-\text{NH}_2$ group in chitosan molecule occurred. The
270 deprotonation could strengthen the interaction between chitosan and ZnS QDs in some degree,
271 which brought about partly fluorescence enhancing. However, the fluorescence intensity began to
272 decrease with the further increase of pH ($\text{pH} > 4.5$), as the solubility of chitosan decreased, which
273 resulted in partly precipitation of the QDs. In the presence of BPA, as illustrated in Fig. 4C, F_0/F
274 is also stable and high in the pH range of 4.0-4.5. Thus, the optimal pH was chosen to be 4.0 for
275 further experiments.

276 To gain the widest linear range and the highest sensitivity of the calibration function, the
277 effect of ZnS QDs concentration on the F_0/F of BPA-ZnS QDs system was further investigated. A
278 relatively low concentration of ZnS QDs can only provide very weak fluorescence emission
279 correspondingly, which is not beneficial for obtaining a wider linear range. With the increase of
280 the ZnS QDs concentration, the fluorescence intensity of the system rises up gradually (not
281 shown). A very high QDs concentration could enlarge the linear range but at the expense of
282 sensitivity. As shown in Fig. 4D, the maximum F_0/F was achieved when the concentration was 1.2
283 $\times 10^{-6} \text{ mol}\cdot\text{L}^{-1}$. Comprehensively considering high sensitivity and wide linear range, a QDs
284 concentration of $1.2 \times 10^{-6} \text{ mol}\cdot\text{L}^{-1}$ (in test sample) was recommended for further research.

285 **3.4 Calibration and sensitivity**

286 As shown in Fig. 5, under the optimal conditions mentioned above, the addition of BPA
287 gradually decreased the fluorescence intensity of the ZnS QDs, so a quantitative determination of
288 BPA based on fluorescence quenching was possible. The inset in Fig. 5 illustrates that F_0/F
289 exhibits a good linear relationship with the concentration of BPA in a wide range from 0.05 to 300
290 $\mu\text{g}\cdot\text{L}^{-1}$, which is well described by a Stern-Volmer (SV) equation with the correlation coefficient
291 of 0.99531:

$$\frac{F_0}{F} = 0.97064 + 0.01431c_{\text{BPA}} \quad (2)$$

292 where c_{BPA} is the concentration of BPA ($\mu\text{g}\cdot\text{L}^{-1}$). The limit of detection (LOD) for BPA in water is
293 $0.08 \mu\text{g}\cdot\text{L}^{-1}$ with the ratio of signal to noise of 3 ($S/N = 3$). The relative standard deviation (RSD)
294 for 6 parallel determinations of a solution containing $25.0 \mu\text{g}\cdot\text{L}^{-1}$ BPA was 1.2%. This indicates
295 that the method can offer good precision for the detection of BPA. Compared with the existing
296 methods (shown in Table S2), a relatively low detection limit was obtained and it was also greatly
297 lower than $30.0 \mu\text{g}\cdot\text{L}^{-1}$, which is the LOD given by the HPLC method according to Chinese
298 National Standard GB/T 23296.16-2009 (Food contact materials-Polymer-Determination of
299 bisphenol A in food simulants-High performance liquid chromatography). Obvious advantages
300 were reflected in the proposed method, such as easy sample pretreatment, short analysis time, low
301 cost and nontoxicity.

303 3.5 Interference studies

304 The fluorescence titration of chitosan-capped ZnS QDs with various coexisting substances
305 was performed to examine the detection selectivity. Table S3 described the influence of coexisting
306 substances on the fluorescence intensity of ZnS QDs with BPA. For coexisting substances, K^+ ,
307 Na^+ , Al^{3+} , Ca^{2+} , Ba^{2+} , NH_4^+ , Mg^{2+} , CO_3^{2-} , SO_4^{2-} , PO_4^{3-} , CH_3COO^- , NO_3^- , Cl^- , Mn^{2+} , glucose,

308 lactose and glycine induced less than $\pm 5\%$ change of the fluorescence intensity of ZnS QDs and
309 the tolerance limits of these substances were more than $12500 \mu\text{g}\cdot\text{L}^{-1}$, at least 500 times than the
310 coexisting BPA concentration, which means these coexisting substances had no interference for
311 detection of $25.0 \mu\text{g}\cdot\text{L}^{-1}$ BPA. Zn^{2+} had a fluorescence enhancement effect at a relative higher
312 concentration since they were adsorbed onto the surface of ZnS QDs and the increase of S surface
313 vacancies improved the defect-related emission of ZnS QDs in some degree. Fe^{3+} , Cu^{2+} , Hg^{2+} and
314 Ag^{+} exhibited effective quenching effect, which is attributed to their strong chemical adsorption
315 onto the ZnS QDs surface. However, the tolerance limits of these ions were at least 5 times of the
316 BPA concentration and greatly higher than their potential concentration present in real samples.
317 Thus, the detecting system herein possessed a good selective fluorescence response toward BPA
318 and it could be applied to determine BPA in real samples.

319 **3.6 Detection of BPA in real samples**

320 The proposed method was applied for the determination of BPA in tap, rain and packaged
321 drinking water. Standard addition method was used to evaluate the analytical performance of the
322 fluorescence sensor and the results were shown in Table 1. It can be clearly seen that the
323 recoveries were in the range of 95.9-105.8% with RSD values between 1.5% and 4.0%, indicating
324 that the fluorescence sensor might be sufficient and satisfactory for BPA detection in these water
325 samples. No BPA was detected in the tap water sample. From one packaged drinking water
326 sample, BPA was detected at a very low amount of $0.19 \mu\text{g}\cdot\text{L}^{-1}$, and for the other, it was not
327 detected. This very low amount of BPA in packaged drinking water may be caused by BPA
328 migration from the packages under unreasonable storage conditions. $0.41 \mu\text{g}\cdot\text{L}^{-1}$ BPA was
329 detected in the rain water sample, which may be due to a very slow BPA migration from domestic

330 garbage and wastewater to the global water cycle.

331 Samples of plastic cups, feeding bottles, microwave lunch boxes and epoxy resin-based
332 bowls with different brands were also inspected. Different ultrasonic and microwave extraction
333 conditions had been investigated. The optimal conditions was selected as 90 °C and 90 min for
334 ultrasonic extraction, and 10 min for microwave extraction since under these conditions the
335 extraction periods were significantly shortened and the extraction effect were equivalent to those
336 under the condition stipulated by GB/T 23296.1-2009. After extraction procedures under the
337 above optimal conditions, leaching solutions of the plastic samples were respectively examined
338 using the proposed method and the results were shown in Table 1. High recoveries from 96.4% to
339 104.3% were obtained for these plastic samples with RSD values between 1.0% and 4.4%. The
340 result demonstrates that the proposed analytical method was also competent for BPA detection of
341 plastic samples. It can be seen that no BPA was detected in the samples of the PP-made plastic
342 products. However, in some PC-made or PC-containing materials, different amounts of BPA could
343 be detected, which illuminates that the employed BPA extraction processes in this assay are very
344 effective.

345 **3.7 Quenching mechanism**

346 Up to now, many quenching mechanisms including energy transfer, charge diverting and
347 surface absorption have been proposed to explain the fluorescence quenching phenomena of QDs.
348 To explore the possible mechanism involved in the interaction between chitosan-capped ZnS QDs
349 and BPA, the UV-vis absorption spectra of BPA, ZnS QDs and ZnS QDs adding BPA were
350 investigated. Shown as curve a in Fig. S2, BPA had no absorption in the wavelength range of
351 300-600 nm, so the quenching effect of BPA on the fluorescence of ZnS QDs is not due to inner

352 filter effect resulting from the absorption of the emission wavelength by BPA. No obvious change
353 was observed from the ZnS QDs absorption spectra before and after adding BPA (curve b and c in
354 Fig. S2) and no perceptible red shift on the maximum emission wavelength can be found in Fig. 5
355 with increasing concentration of BPA, which indicates that the presence of BPA mainly influences
356 the surface status and not the size of the ZnS QDs. Generally, in alkaline environment, the process
357 of complexation reaction between BPA and Zn^{2+} on ZnS QDs surface may occur. While the
358 current ZnS QDs-BPA system is weak acidic, there is little probability of the complexation
359 reaction. The zeta potential of BPA in the weak acidic solution was also measured to be 23.0 mV
360 (Fig. S1B). Since both BPA and ZnS QDs possessed positive charges, there is no electrostatic
361 attractive interaction between them. Thus, the quenching may be due to the hydrogen bonding
362 between BPA and chitosan on the surface of the QDs (Scheme 1D). BPA could bind to the surface
363 of chitosan-capped ZnS QDs like a cap through the hydrogen-bond interaction between $-OH$ of
364 BPA and $-NH_2/-OH$ of chitosan.³² The hydrogen bonds lead chitosan molecules to partly peel off
365 from the surface of the ZnS QDs, then the surface changes induced the fluorescence quenching of
366 the ZnS QDs.²¹

367 **4. Conclusion**

368 In summary, with chitosan as capping and stabilizing agent, water-soluble ZnS QDs were
369 easily prepared. By using the nontoxic ZnS QDs as fluorescence probe, a novel and eco-friendly
370 technique for rapid BPA detection with high sensitivity and selectivity was developed based on
371 the quenching effect of BPA on the fluorescence emission of ZnS QDs. The possible quenching
372 mechanism is due to the surface change of ZnS QDs, induced by hydrogen bonding between BPA
373 and chitosan on the surface of ZnS QDs. The factors affecting both the synthesis of

374 chitosan-capped ZnS QDs and the fluorescence detection for BPA were also examined. Under the
375 optimal assay conditions, a relatively wide linear range (from 0.50 to 300 $\mu\text{g}\cdot\text{L}^{-1}$) and low
376 detection limit (0.08 $\mu\text{g}\cdot\text{L}^{-1}$) were obtained. Most common coexisting substances hardly interfered
377 with the determination of BPA. The proposed method was successfully applied to the recognition
378 of BPA in water and plastic samples, and simplicity, rapidity, high sensitivity and low cost was
379 exhibited in detection process. Thus, it appears to be a promising candidate for on-site rapid
380 screening of BPA contamination in water and plastic samples.

381 **Acknowledgements**

382 This work was financially supported by the National Natural Science Foundation of China
383 (No. 20905031), the Natural Science Foundation of Jilin Province (No. 201215024) and
384 Innovation Projects of Science Frontiers and Interdisciplinary of Jilin University.

385 **References**

- 386 1 C. A. Staples, K. Woodburn, N. Caspers, A. T. Hall and G. M Klecka. *Human Ecol. Risk Assess.*, 2002, **8**,
387 1083-1105.
- 388 2 D. A. Crain, M. Eriksen, T. Iguchi, S. Jobling, H. Laufer, G. A. LeBlanc and L. J. G. Jr, *Reprod. Toxicol.*, 2007,
389 **24**, 225-239.
- 390 3 L. N. Vandenberg, R. Hauser, M. Marcus, N. Olea and W. V. Welshons, *Reprod. Toxicol.*, 2007, **24**, 139-177.
- 391 4 N. K. Wilson, J. C. Chuang, M. K. Morgan, R. A. Lordo and L. S. Sheldon, *Environ. Res.*, 2007, **103**, 9-20.
- 392 5 H. H. Le, E. M. Carlson, J. P. Chua and S. M. Belcher, *Toxicol. Lett.*, 2008, **176**, 149-156.
- 393 6 E. Carlsen, A. Giwercman, N. Keiding and N. E Skakkebaek, *Environ. Health Perspect.*, 1995, **103**, 137-139.
- 394 7 X. H. Long, R. Steinmetz, N. Ben-Jonathan, A. Caperell-Grant, P. C. M. Young, K. P. Nephew and R. M.
395 Bigsby, *Environ. Health Perspect.*, 2000, **108**, 243-247.

- 396 8 X. W. Tan, Y. X. Song, R. P. Wei and G. Y. Yi, *Chin. J. Anal. Chem.*, 2012, **40**, 1409-1414.
- 397 9 A. Motoyama, A. Suzuki, O. Shiota and R. Namba, *Rapid Commun. in Mass Spectrom.*, 1999, **13**, 2204-2208.
- 398 10 M. K. R. Mudiam, R. Jain, V. K. Dua, A. K. Singh, V. P. Sharma and R. C. Murthy, *Anal. Bioanal. Chem.*,
399 2011, **401**, 1695-1701.
- 400 11 Y. Lu, J. R. Peterson, J. J. Gooding and N. A. Lee, *Anal. Bioanal. Chem.*, 2012, **403**, 1607-1618.
- 401 12 S. X. Zhong, S. N. Tan, L. Y. Ge, W. P. Wang and J. R. Chen, *Talanta*, 2011, **85**, 488-492.
- 402 13 C. M. Yu, L. L. Gou, X. H. Zhou, N. Bao and H. Y. Gu, *Electrochim. Acta*, 2011, **56**, 9056-9063.
- 403 14 C. Lu, J. G. Li, Y. Yang and J. M. Lin, *Talanta*, 2010, **82**, 1576-1580.
- 404 15 G. F. Li, S. Morita, S. Ye, M. Tanaka and M. Osawa, *Anal. Chem.*, 2004, **76**, 788-795.
- 405 16 Z. L. Mei, H. Q. Chu, W. Chen, F. Xue, J. Liu, H. N. Xu, R. Zhang and L. Zheng, *Biosens. Bioelectron.*, 2013,
406 **39**, 26-30.
- 407 17 K. Hegnerova, M. Piliarik, M. Steinbachova, Z. Flegelova, H. Cernohorska and J. Homola, *Anal. Bioanal.*
408 *Chem.*, 2010, **398**, 1963-1966.
- 409 18 X. Y. Liu, C. Nakamura, I. Tanimoto, S. Miyake, N. Nakamura, T. Hirano and J. Miyake, *Anal. Chim. Acta*,
410 2006, **578**, 43-49.
- 411 19 J. Fan, H. Q. Guo, G. G. Liu and P. G. Peng, *Anal. Chim. Acta*, 2007, **585**, 134-138.
- 412 20 Y. Kim, J. B. Jeon and J. Y. Chang, *J. Mater. Chem.*, 2012, **22**, 24075-24080.
- 413 21 R. Kuang, X. Kuang, S. Y. Pan, X. D. Zheng, J. C. Duan and Y. Q. Duan, *Microchim. Acta*, 2010, **169**,
414 109-115.
- 415 22 X. Wang, H. L. Zeng, Y. L. Wei and J. M. Lin, *Sens. Actuators ,B*, 2006, **114**, 565-572.
- 416 23 S. A. O. Gomes, C. S. Vieira, D. B. Almeida, J. R. Santos-Mallet, R. F. S. Menna-Barreto, C. L. Cesar and D.
417 Feder, *Sensors*, 2011, **11**, 11664-11678.

- 418 24 H. Li, M. Y. Li, W. Y. Shih, P. I. Lelkes and W. H. Shih, *J. Nanosci. Nanotechnol.*, 2011, **11**, 3543-3551.
- 419 25 Z. Li, Y. M. Du, Z. L. Zhang and D. W. Peng, *React. Funct. Polym.*, 2003, **55**, 35-43.
- 420 26 M. Sharma, S. Singh and O. P. Pandey, *J. Appl. Phys.*, 2010, **107**, 104319.
- 421 27 A. Jaiswal, P. Sanpui, A. Chattopadhyay, and S. S. Ghosh, *Plasmonics*, 2011, **6**, 125-132.
- 422 28 J. Q. Zhuang, X. D. Zhang, G. Wang, D. M. Li, W. S. Yang and T. J. Li, *J. Mater. Chem.*, 2003, **13**, 1853-1857.
- 423 29 S. Chowdhury, A. M. P. Hussain, G. A. Ahmed, F. Singh, D. K. Avasthi and A. Choudhury, *Mater. Res. Bull.*,
424 2008, **43**, 3495-3505.
- 425 30 A. T. R. Williams, S. A. Winfield and J. M. Miller, *Analyst*, 1983, **108**, 1067-1071.
- 426 31 C. H. Song, Y. T. Li, J. Li, Y. J. Wei, Y. Z. Hu and Y. Wei, *Spectrosc. Spect. Anal.*, 2008, **28**, 169-173.
- 427 32 T. I. Chanu and D. P. S. Negi, *Chem. Phys. Lett.*, 2010, **491**, 75-79.
- 428

429 **Figure Captions**

430 Scheme 1. (A) The molecular structure of BPA. (B) The molecular structure of chitosan. (C) Formation process of
431 chitosan-capped ZnS QDs. (D) The proposed mechanism for the quenching effect of BPA on the fluorescence of
432 chitosan-capped ZnS QDs.

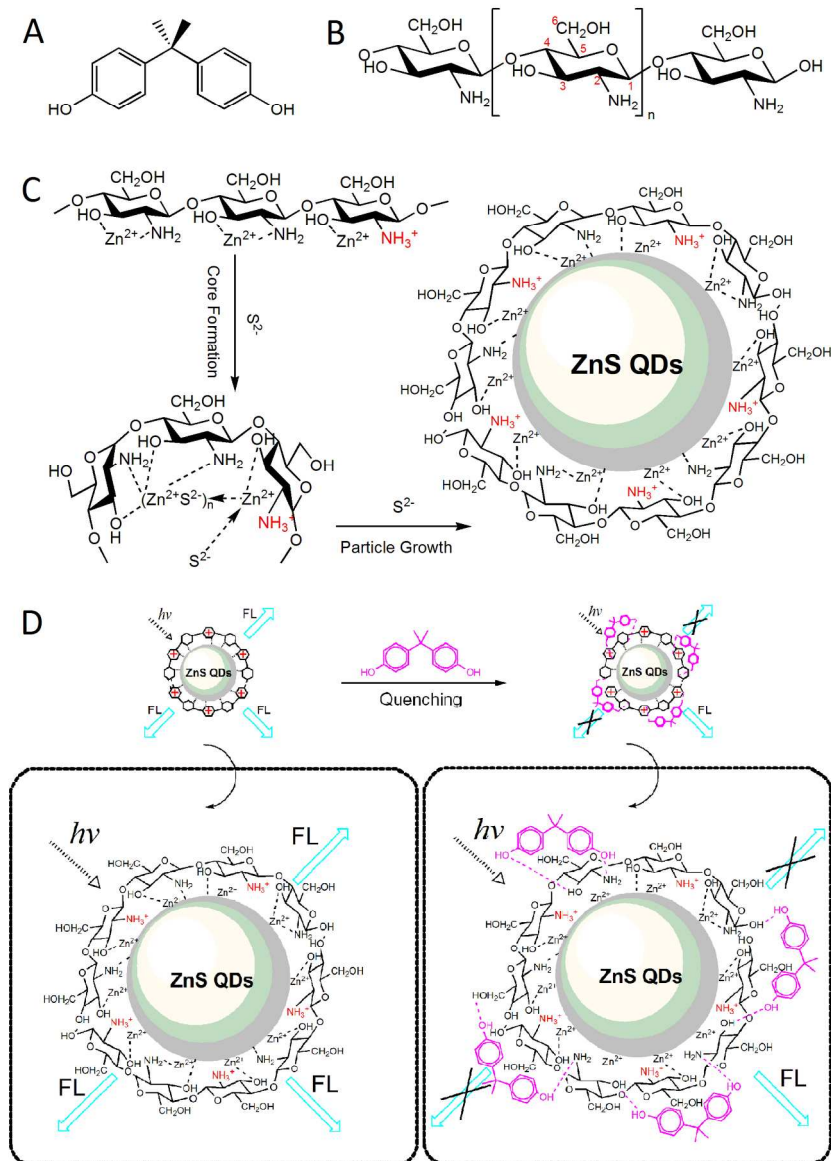
433 Fig. 1. FT-IR spectra of pure chitosan (A) and chitosan-capped ZnS QDs (B).

434 Fig. 2. (A) The absorption spectrum (a) and fluorescence emission spectrum (b) of the as-prepared ZnS QDs, and
435 the digital photographs of the ZnS QDs solution under daylight (c) and a 308 nm UV lamp (d). (B) HRTEM
436 images of the ZnS QDs.

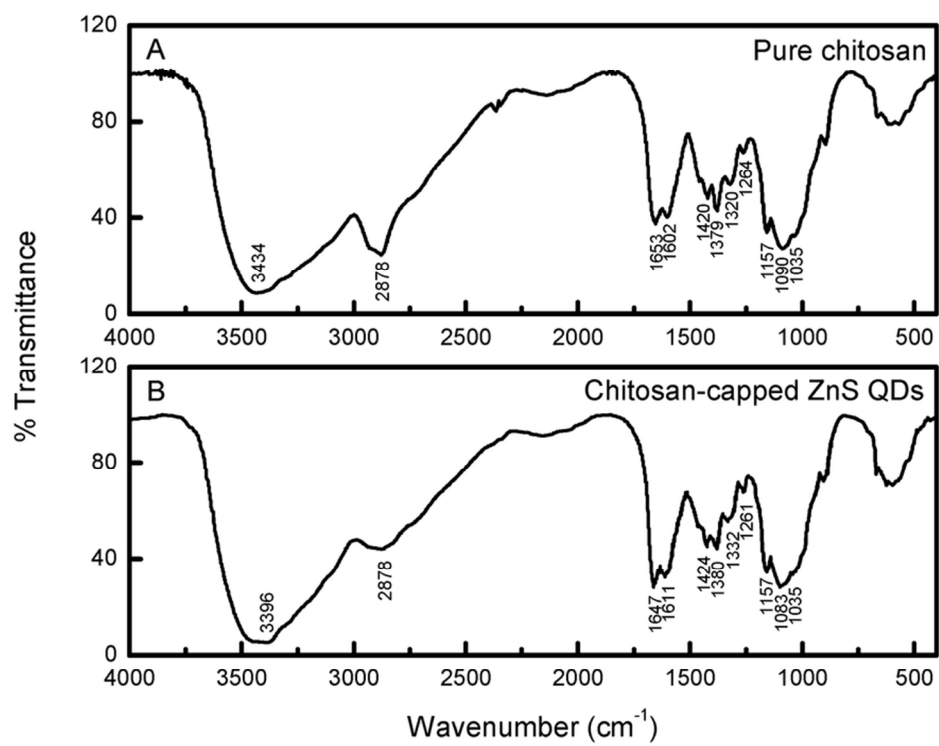
437 Fig. 3. The fluorescence emission spectra of $1.2 \times 10^{-6} \text{ mol}\cdot\text{L}^{-1}$ ZnS QDs in the absence (a) and presence (b) of 150
438 $\mu\text{g}\cdot\text{L}^{-1}$ BPA.

439 Fig. 4. (A) Variation of F_0/F versus the reaction time for ZnS QDs after addition of BPA. (B) Effect of pH on the
440 fluorescence intensity of ZnS QDs. (C) Effect of pH on F_0/F with the presence of BPA. (D) Effect of ZnS QDs
441 concentration on F_0/F with the presence of BPA. ZnS QDs for A, B and C, $1.2 \times 10^{-6} \text{ mol}\cdot\text{L}^{-1}$; BPA for A and C,
442 $150 \mu\text{g}\cdot\text{L}^{-1}$, for D, $50 \mu\text{g}\cdot\text{L}^{-1}$.

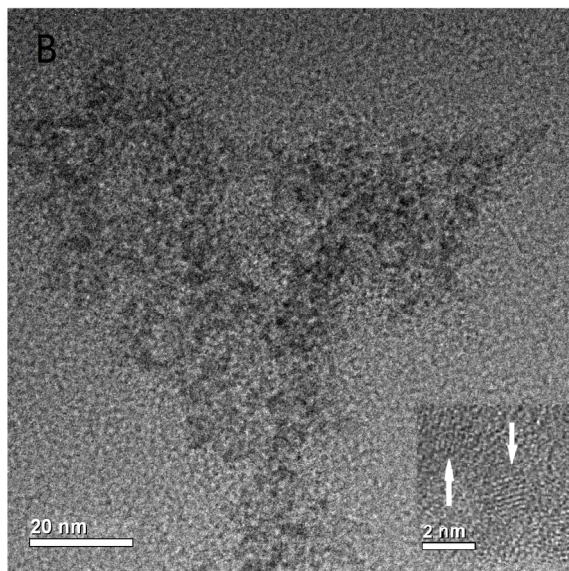
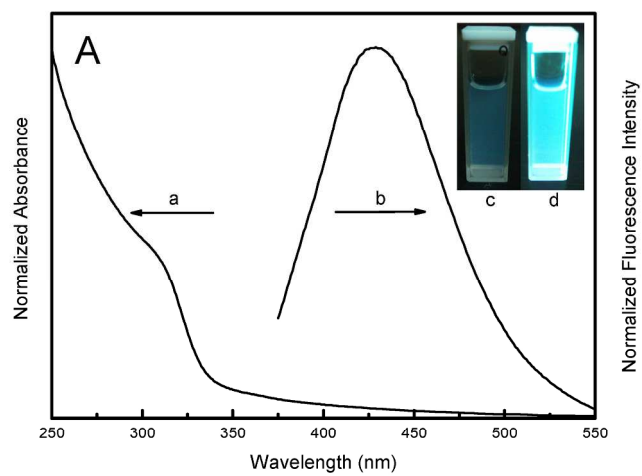
443 Fig. 5. Fluorescence emission spectra of ZnS QDs in the presence of increasing concentrations of BPA. The
444 concentration of BPA in samples (a)-(o) is 0, 0.50, 0.83, 1.66, 3.33, 8.33, 13.3, 16.6, 25.0, 33.3, 50.0, 100, 150,
445 200 and $300 \mu\text{g}\cdot\text{L}^{-1}$, respectively. ZnS QDs, $1.2 \times 10^{-6} \text{ mol}\cdot\text{L}^{-1}$. The inset shows the calibration curve of F_0/F versus
446 the concentration of BPA.



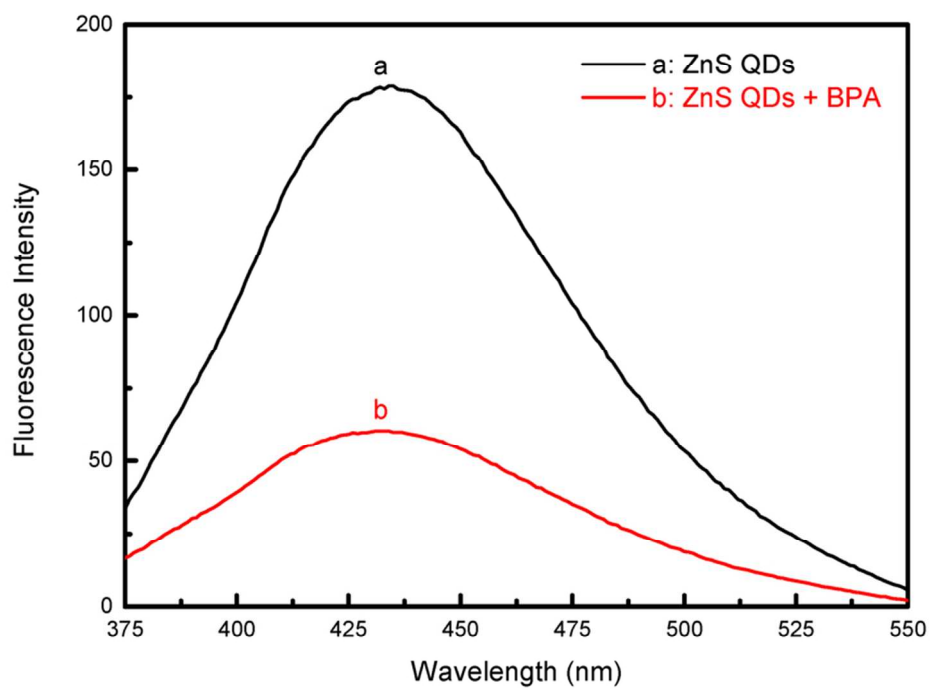
212x297mm (300 x 300 DPI)



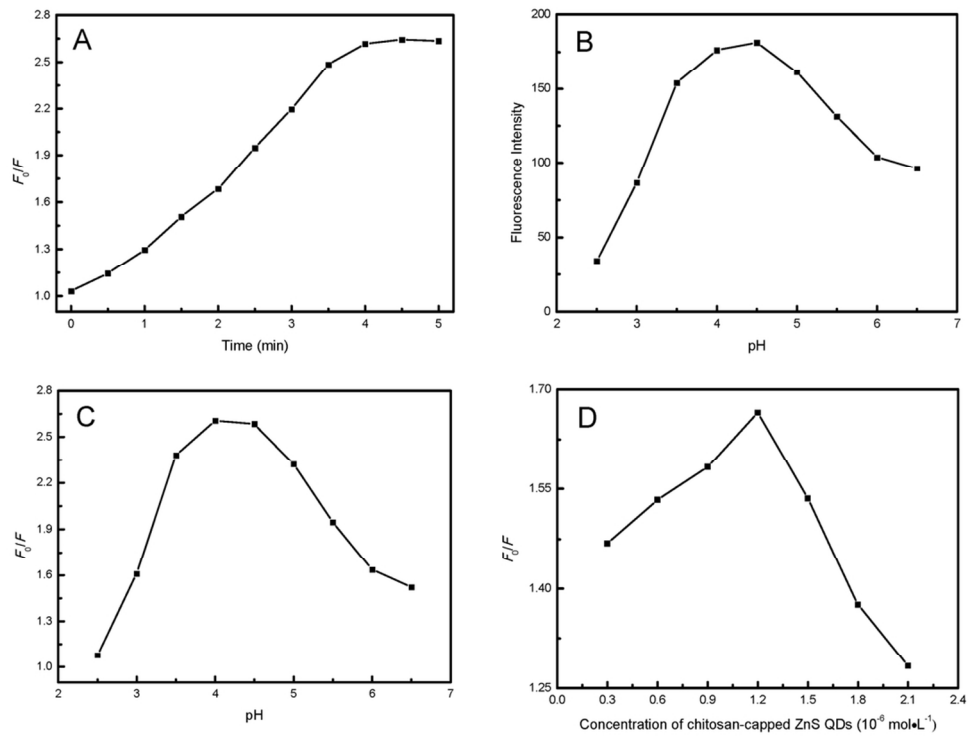
79x63mm (300 x 300 DPI)



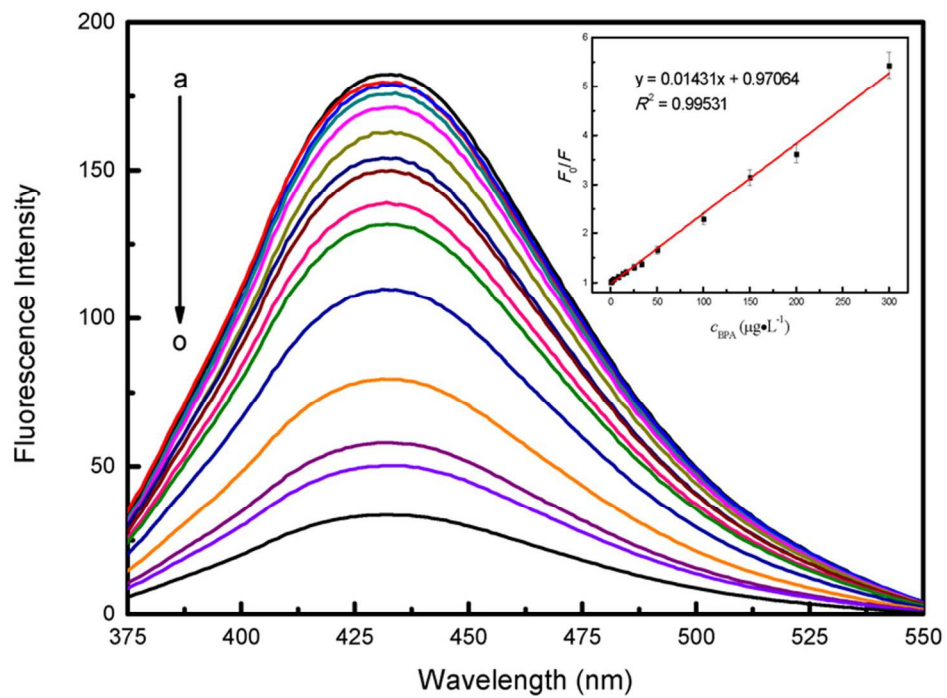
179x315mm (300 x 300 DPI)



78x59mm (300 x 300 DPI)



96x74mm (300 x 300 DPI)



74x54mm (300 x 300 DPI)

Table 1 Concentrations and recoveries of BPA in various water samples and plastic leaching solutions

Sample	Background ($\mu\text{g}\cdot\text{L}^{-1}$) ^a	Spiked ($\mu\text{g}\cdot\text{L}^{-1}$)	Found ($\mu\text{g}\cdot\text{L}^{-1}$) ^a	Recovery (%)	RSD (% , $n = 6$)
Tap water	ND ^b	2	1.98	99.0	2.5
		10	10.17	101.7	2.2
		50	49.36	98.7	3.0
Rain water	0.41	2	2.55	105.8	4.0
		10	10.79	103.7	2.6
		50	51.72	102.6	3.1
Packaged drinking water 1	ND	2	2.07	103.5	1.6
		10	9.90	99.0	2.1
		50	50.99	102.0	1.9
Packaged drinking water 2	0.19	2	2.10	95.9	2.3
		10	10.34	101.5	1.5
		50	51.46	102.5	3.3
Leaching solution: plastic cup 1 (PC)	10.46	2	12.15	97.5	3.6
		10	20.86	102.0	2.3
		50	61.70	102.1	2.0
Leaching solution: plastic cup 2 (PP ^c)	ND	2	2.07	103.5	2.6
		10	9.83	98.3	1.8
		50	48.93	97.9	3.2
Leaching solution: feeding bottle 1 (PC)	22.55	2	24.13	98.3	2.0
		10	32.92	101.1	2.4
		50	72.10	99.4	3.2
Leaching solution: feeding bottle 2 (PP)	ND	2	1.97	98.5	4.1
		10	10.36	103.6	3.0
		50	52.14	104.3	2.7
Leaching solution: microwave lunch box 1 (PP)	ND	2	2.04	102.0	3.7
		10	9.89	98.9	1.7
		50	51.24	102.5	1.9
Leaching solution: microwave lunch box 2 (PET ^d + PC)	1.58	2	3.55	98.1	2.2
		10	11.64	103.8	2.4
		50	51.61	101.9	1.0
Leaching solution: epoxy resin-based bowl 1	39.21	2	41.99	102.0	2.8
		10	50.28	102.7	3.8
		50	90.47	103.2	2.3
Leaching solution: epoxy resin-based bowl 2	3.05	2	5.02	99.0	1.9
		10	13.12	102.3	3.2
		50	52.94	96.4	4.4

^a Mean of six measurements.^b Not detected.^c PP: polypropylene.^d PET: polyethylene terephthalate.

Table of Contents Entry

Quantitative detection of BPA in water and plastic samples was developed based on fluorescence quenching of eco-friendly chitosan-capped ZnS QDs.

